CHALMERS
UNIVERSITY OF TECHNOLOGY

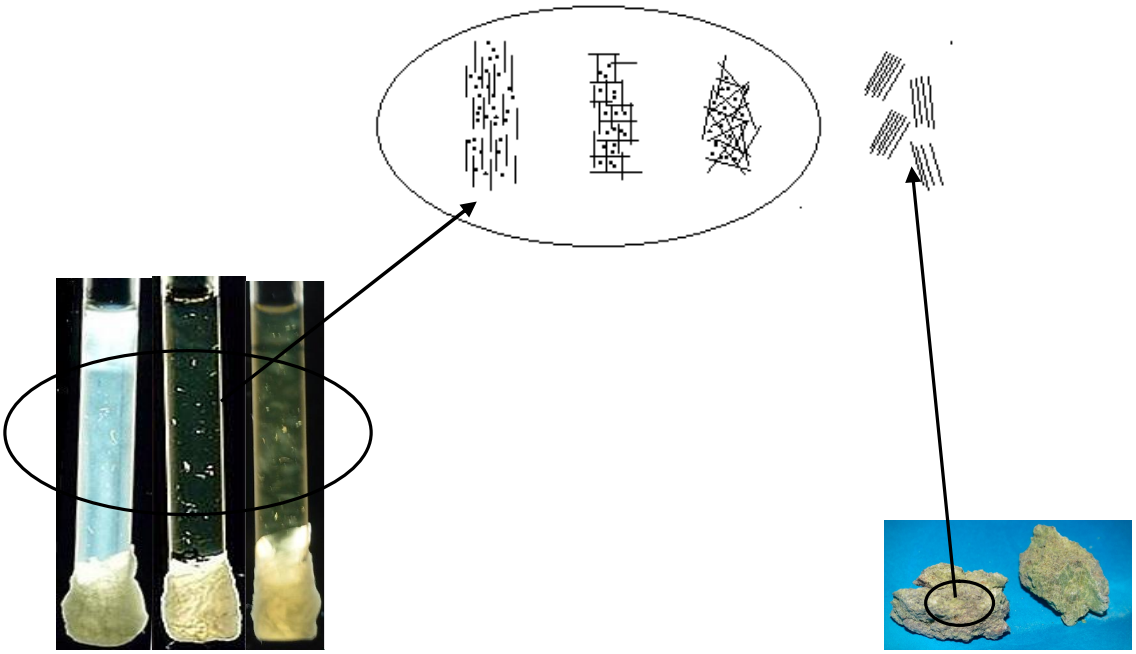

Magnetic alignment and phase behavior of nanoclay dispersions after *in situ* salt formation

YUMAN LI

Division of Applied Surface Chemistry
Department of Chemical and Biological Engineering
CHALMERS UNIVERSITY OF TECHNOLOGY
Gothenburg, Sweden, 2014

MASTER'S THESIS

Magnetic alignment and phase behavior of nanoclay dispersions after *in situ* salt formation

by Yuman Li

30 hp Master's thesis within the Nanotechnology program

Division of Applied Chemistry

Department of Chemical and Biological Engineering,

Chalmers University of Technology, Gothenburg,

Sweden, August, 2014

Supervisor: Christoffer Abrahamsson (PhD student), Applied Chemistry,

Department of Chemical and Biological Engineering,

Chalmers University of Technology

Examiner: Michael Persson (Adjunct Professor), Department of Chemical and Biological Engineering, Applied Chemistry, Chalmers University of Technology and Innovation Manager, Akzo Nobel PPC

Abstract

Nanotechnology with application in nanomaterials and colloidal dispersions is of growing relevance both in fundamental as well as applied research. Anisotropic particles such as clay sheets have been especially promising as these can improve the mechanical and gas/liquid permeability properties when dispersed in a matrix material to form a composite. Due to such particles enormous surface to volume ratios and large aspect ratios, they are common rheological modifiers in processes ranging from food production to oil well drilling. This thesis aimed to find the relationship between magnetic alignment, and clay and salt concentration. In this study, the clay concentration did not determine which sample that aligned in the investigated concentration range (0-0.8 vol%). Instead salt concentration was the factor dominating the alignment. At a salt concentration of 10^{-3} M NH_3HCO_3 and below the samples could align in an 11.7 Tesla magnetic field. Above this salt concentration the samples did not align or aligned very slowly. The rheological properties, as indicated by an inverted tube test, were poor predictors of which samples would magnetically align. One important conclusion is therefore that it is not possible to say that a more viscous clay sample will magnetically align slower than a less viscous sample.

The thesis work also aimed to formulate new types of latex-clay composite films to study the effect of clay alignment in the film on the film permeability. Unfortunately the formulation of the latex/clay composites failed as it was hard to achieve reproducible gelation.

Keywords: nanocomposite, nontronite clay, exfoliated clay, magnetic alignment, phase behavior

Table of content

1 Introduction

Nanotechnology with application to nanomaterials is of growing relevance both in fundamental as well as applied research. Nanoparticles have enormous surface to volume ratios which gives them very different properties compared to a bulk structure made from the same material [1-3]. Moreover, these nanoparticles can be designed to self-assemble into nanostructures with unique material characteristics [4]. The introduction of nanostructured anisotropy that spans into the macroscale is a powerful way of enhancing certain material properties, for example mechanical strength [5, 6], diffusion and flow of liquid through porous materials [7] and optical properties [8].

A group of nanostructured materials that occur in nature is the clays. Clay consists of inorganic crystalline sheets of mixed shapes that are a few nanometer thick and up to 2000-3000 nm wide [9, 10]. Clay sheets in liquid dispersions are typically stacked and packed like pages in a book, yet under certain conditions the individual sheets can be dispersed into individual sheets, forming an exfoliated dispersion [11]. In the oil industry clay dispersions play an important role as lubricants and sealants of oil wells when oil and gas is to be extracted from underground reservoirs. For such applications a good understanding of the colloidal stability and especially the rheology is essential. The ground around the wells contains regions of varied pH and salt concentration, all of which affect the colloidal behavior. A better understanding of the clays response to factors present in such environments is therefore of interest [12].

1.1 Aim

The first aim of the project was to investigate how clay-clay interactions within aqueous nontronite clay dispersions and gels are affected by clay and salt concentration. This was done by observing: the overall sample colloidal phase behavior, the bulk rheology by an “inverted tube test”, and the microrheology by investigating the magnetic alignment of samples in strong magnetic fields.

The second aim was to use a sol-gel method to synthesize composite films from colloidal nontronite clay and latex particles in the presence or absence of a magnetic field. These films were then to be used to study the influence of different states of clay alignment on liquid permeability of the films.

1.2 Limitations

There are some limitations in the scope of the investigation. In the nontronite clay-urea/urease experiments only one clay and salt type was investigated. The only formulation process studied was the sol-gel method. Also, only the urea/urease *in situ* salt formation methods was investigated for this system.
In the clay-latex system only one clay type was investigated and only two different *in situ* salt formation methods. The following *in situ* methods were investigated: the urea/urease and the glucono-δ-lactone/$CaCO_3$ methods.

2 Background

2.1 Colloidal particles and dispersions

Particles that have at least one dimension in the size range 10^{-9}-10^{-6} m can be defined as colloidal particles [13]. When particles are in the colloidal size range they can under some conditions form stable dispersions that do not sediment. The particles are in constant Brownian motion as they diffuse in the dispersions [14]. Important factors affecting the colloidal stability of the particles are particle concentration, size and shape, surface chemistry and surface charge, hydrophobicity and hydrophilicity [15, 16, 17]. Some of these factors are influenced by the properties of the surrounding medium such as type of solvent, salt concentration or pH [15, 18]. In a charge stabilized colloidal system, particles electrostatically repel each other mainly due to surface charges [19].

The Brownian motion of particles can be described by the Stokes-Einstein equation (Equation 1), where k the Boltzmann constant, T the absolute temperature, η the dynamic viscosity, α the radius of the particles [20]. The equation could also be applied to plate shaped particles such as clays, assuming a hydrodynamic diameter [21].

$$D = \frac{kT}{6\pi\alpha\eta} \quad \text{.....} \quad \text{.....[Equation 1]}$$

2.2 Interaction between charged particles

2.2.1 Charges on the surface

Charged colloidal particles in dispersions are surrounded by a cloud of ions that form what is called an electric double layer. The ions will not be distributed uniformly throughout the liquid phase, instead they will be more concentrated near the charged colloidal surface. Figure 2 shows the counter and co-ions that are located closest to the surface in the stern-layer. Outside the stern layer alternative layers of oppositely charged ions are located, however the charges gets increasingly uniformly mixed at increasing distance from the surface. This part of the electric double layer is often referred to as the Gouy-Chapman Double Layer [22].

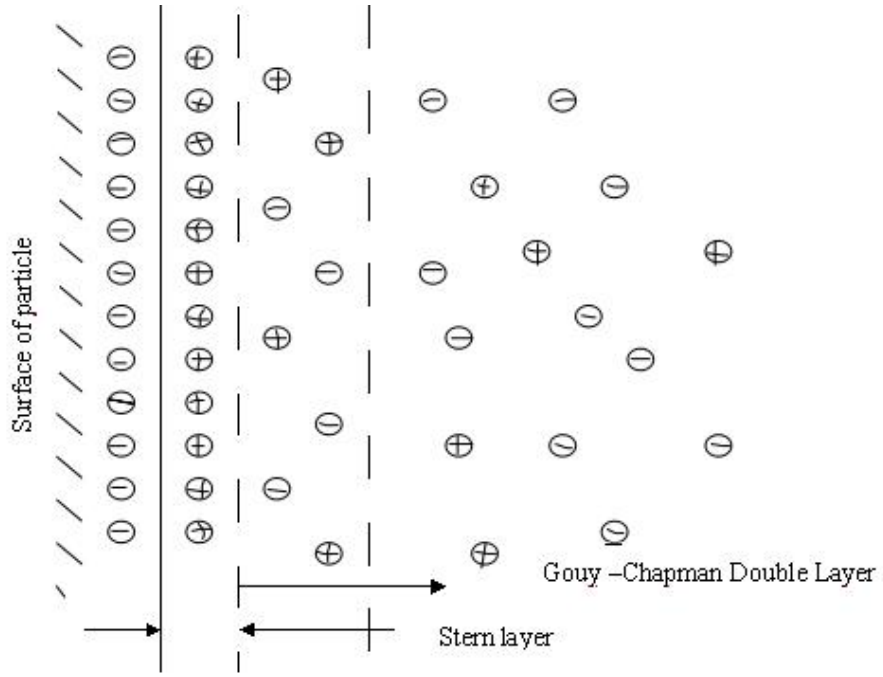

Figure 1 Schematic of the electric double layer [22].

2.2.2 DLVO theory

The DLVO (Derjaguin, Landau, Verwey and Overbeek) theory describes colloidal stability and interactions between colloidal particles in a liquid environment. There are several forces that affect the particle interactions, including electrostatic interactions and Van der Waals interactions [23]. For example, similarly charged particles will repel each other, but Van der Waals forces will cause attraction between them.

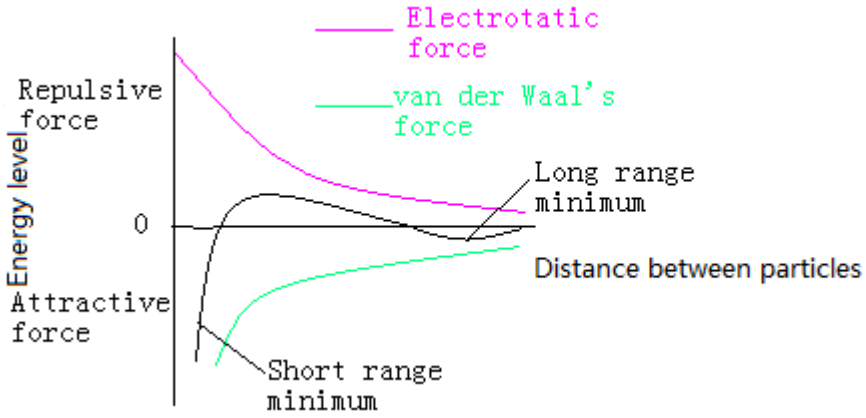

Figure 2 Schematic of forces affecting the particle-particle interaction (energy level) as a function of the distance between the particles [24].

The energy barrier in the black curve in Figure 2 will keep the particles from aggregating when the sol is stable. This barrier can be several times greater than the kinetic energy of the

particles and under these conditions the particles will not aggregate. Energy minimums are observed where the total net energy corresponds to attraction on both sides of the energy maximum. The particles can form loose flocculates at distances corresponding to the long range energy minimum and such aggregates can sometimes be re-dispersed. However, at the short range minimum the particles tend to aggregate irreversibly [11].

2.2.3 Colloidal stability

There are many factors that influence colloidal stability in particle dispersions/sols and these factors will affect the balance between repulsive and attractive forces. In that context the key criterion that needs to be fulfilled for a sol to be stable is that an energy barrier is needed to keep the particles apart. Particle size is important as small particles tend to remain in dispersions due to Brownian motion counteracting gravitationally driven sedimentation. Particle surface charges often stabilize the particles by providing a repulsive force between particles and thereby making particle-particle aggregation less likely [14].

The addition of ions can screen the particle surface charges, or in DLVO theory terms, the additions of ions lower the energy barrier for particle-particle aggregation. Different types of ions will have different effect on the stability and divalent ions such as Ca^{2+} usually screens more efficiently compared to monovalent ions such as Na^{+} [25]. Increasing the ion concentration in the dispersion will compress the electric double layer and reduce the particle-particle repulsion so that the energy barrier is decreased, which causes particle aggregation.

Another type of colloidal stability mechanism is steric repulsion. This effect is often present in colloidal systems where the particle surfaces are covered by grafted or adsorbed polymer molecules. There are two effects that cause this type of repulsion, both the osmotic effect caused by the high concentration of chain elements in the region of overlap, and a volume restriction effect caused by of the loss of possible polymers strand conformations in the narrow space between two particles that are close to each other [26].

2.3 Interaction between clay and water molecules

Water is a polar molecule that together with other water molecules will self-organize close to the negatively charged faces and positively charged edges of the clay sheets. A clay sheet is schematically illustrated in Figure 3 [27]. Fully exfoliated clay sheets that have been delaminated into individual sheets can absorb much larger amounts of water compared to aggregated bulk clay that has much less accessible surface [28]. Different types of clays have different surface charges and hence different amounts of cations close to their surfaces, which in turn affect the polarization of water molecular. In effect the water will form a 3-4 water layer thick film of immobilized water on the clay surfaces [7]. The surface of clays such as montmorillonite, which is a close relative to nontronite, often behaves as a weak acid [29]. This is mainly because of the deprotonation of hydroxylgroups, located to some extent on the faces, but mainly on the edges of the clay particles [30].

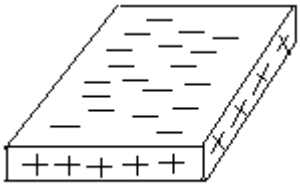

Figure 3 Schematic of clay sheet and the location of charges.

2.4 Clay sheet alignment in magnetic field

Nontronite clay sheets are rich in iron ions in the octahedral layer which makes clay particles in dispersion susceptible to magnetic field alignment [7]. The magnetic susceptibility of the clay particles, described as the clay sheets response to a magnetic field, can be affected by shape, size fraction, concentration of clay and to some extent thermal diffusion [11, 31, 33]. The magnetic torque forces the magnetic moment of the clay particles to align in the magnetic field direction [32]. Nematic phases have been found to be easier to magnetically align as these phases make the collective movement the particles easier [11]. The characteristics of nematic phases are further discussed below. The dispersions transition from an isotropically oriented state to an aligned state can be visualized between crossed polarizers as the samples goes from an optically dark, to a birefringent bright appearance, respectively.

2.5 Clay and its dispersions

Clay consists of small crystalline sheet-like particles of various shapes that in the case of nontronite clay is 1 nm thick and between 10 to 2000 nm wide [7]. The crystal structure of nontronite has an octahedral layer sandwiched between two tetrahedral silica layers and each layer contains metal ions located in the octahedral interlayer. Figure 4 illustrate the crystalline structure of the clay sheets. Different substances can penetrate the interlayer between the clay sheets and in the presence of water the cations in the inter-layer can be hydrated. Such processes help with the clay exfoliation [34].

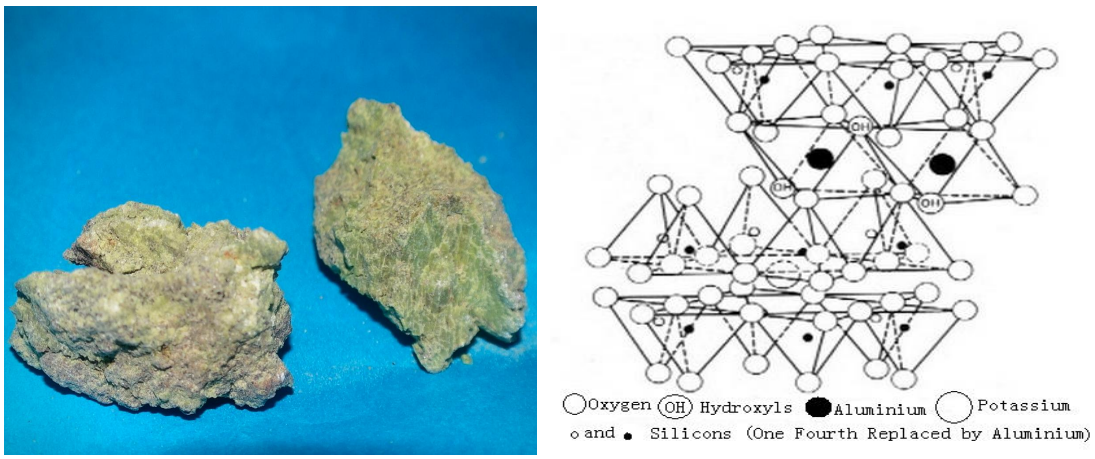

Figure 4 The left image show lumps of dry nontronite clay that was used for this thesis, and the right figure show a schematic model of the clay crystal structure (with permission from Mc Graw Hill education) [35].

The replacement of ions in the crystal structure makes the clay surface charge negative. For instance if Al^{3+} replace Si^{4+} there will be one extra negative charge that will give the clay a net negative charge. The charges of the chemical groups protruding at the edges of the clay particle can be either positive or negative depending on the dispersion pH [30].

2.6 Clay dispersion and gel phase behavior

A gel is a network spanning system that binds the water that it contains and that has solid like properties. At the turning point from solution to gel the viscosity of the system usually rises quickly just before gelation. Two common gel formation mechanisms are the physical and chemical mechanisms. Physical gelation tend to be reversible and to be caused by physical cross-links, such as hydrogen or ionic bonding, microphase separation [36] or excluded volume induced close packing [11]. On the other hand, chemical gelation tends to be an irreversible process caused by reacting monomers or cross-linking polymer strands that form a network [37].

By increasing the anisotropic particle concentration in a liquid, different types of phases form. At low particle concentration the phase is isotropic, but at medium to high concentration it becomes nematic (in some cases) and at high concentration it gels. In nematic phases, and sometimes in the birefringent gel phase, the particles have a higher degree of parallel alignment relative to each other. The transition from an isotropic to nematic transition is energetically favorable because the orientational entropy decrease is compensated by the gain in excluded volume interactions [7].

Specifically for nontronite, Michot and co-workers showed that nontronite clay form liquid phases at a low electrolyte concentration of 10^{-4} M NaCl that are isotropic below 0.6 vol% clay, biphasic between 0.6 and 0.8 vol%, and a fully nematic between 0.8-0.83 vol% clay. Above 0.83 vol% clay, birefringent gel phases were formed [11]. The onset of these phase transitions in nontronite are affected by electrolyte concentration, the size of the clay

sheets,and the ratio between diameter and the thickness of the clay sheets [38]. Abrahamsson and colleagues have shown that gelation can take place in nontronite clay dispersions at least down to a clay concentration of 0.5 vol%, at a NH_4HCO_3 salt concentration of 1 M [7].

Gels or flocs of clay particles are often formed in the presence of salt. In these phases the clay sheets often arrange in an edge to face configuration, called a “house of cards” structure. However, just increasing the clay concentration can result in gelation even in the absence of salt as the system becomes close packed [39].

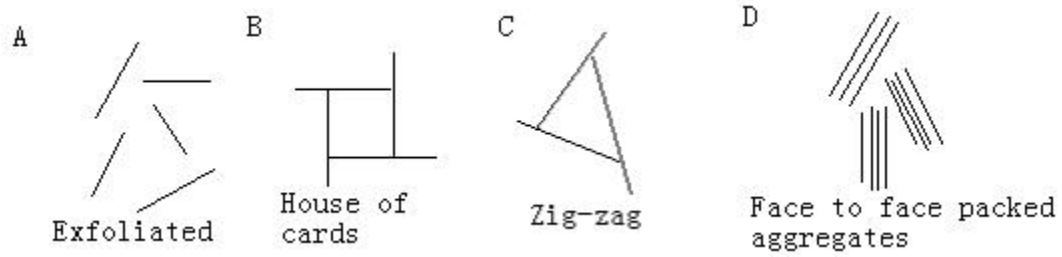

Figure 5 Clay dispersions and gel phases.

The nontronite aggregated phases are organized in different ways depending on the salt concentration. A small addition of salt result in a decrease in the yield stress and viscosity compared to when no salt is added. This can be attributed to a decrease of the effective volume of the clay particles due to screening of the electric double layer by salt ions. This makes it easier for the clay sheets to move which results in shorter relaxation times. At this salt concentration the clay particles are not aggregated but instead interact with each other through mutual repulsion. However, edge-to-face flocculation starts to play a role at low-moderate salt concentrations as the negatively charged faces of one clay sheet interact with the positively charged edges of another clay sheet. These aggregates flocculate relatively fast and usually show no flow birefringence. ‘Zig-zag’ ribbon like structures or even lamellar face-to-face packing of the clay sheets, which are shown in Figure 5C and Figure 5D, tend to occur at moderate-high salt concentration and these phases usually show flow birefringence and relatively dense sediments [40, 41].

3 Techniques description

There are several experimental techniques used in this thesis, for example birefringence observations between crossed polarizers, an inverted tube test that gives an indication of the samples rheological properties and resistivity measurements that was used to try to quantitatively quantify how the structure changed because of magnetic alignment.

3.1 Crossed polarizer observations

Optical polarizers have slits that can filter unpolarized light so that linearly polarized light comes through the filter. If the slit of a second polarizer is oriented perpendicular to the first polarizer no light will go through the second polarizer as shown in the Figure 6. However, if a

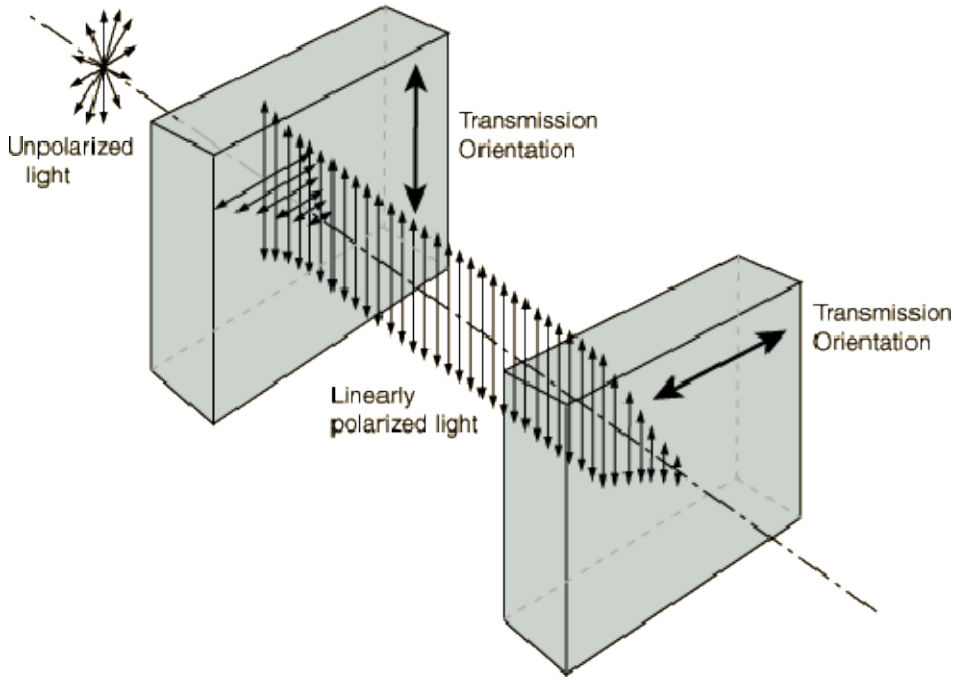

Figure 6 Linearly polarized light is passing through the first polarizer but not the second as the second polarizer has the slit orientation perpendicular to the first (with permission from Hyperphysics project) [44].

sample is inserted between the filters at a 45° angle relative the first slit, light will also pass through the second filter. This usually means that the sample is birefringent which could mean that the sample have an anisotropic alignment in its microstructure that interact with visible light [42, 43].

3.2 Inverted tube test

The rheology of the samples where probed be an "inverted tube test" [45]. In this test the gravity induced movement of the sample inside the tube is visually assessed when inverting the tube. Samples with high viscosity will tend to flow slowly or not move at all as illustrated in the Figure 7. This test was used to asses if the sample was a dispersion or a gel. The method provides an indirect measurement of the strength of the particle-particle interaction in the sample.

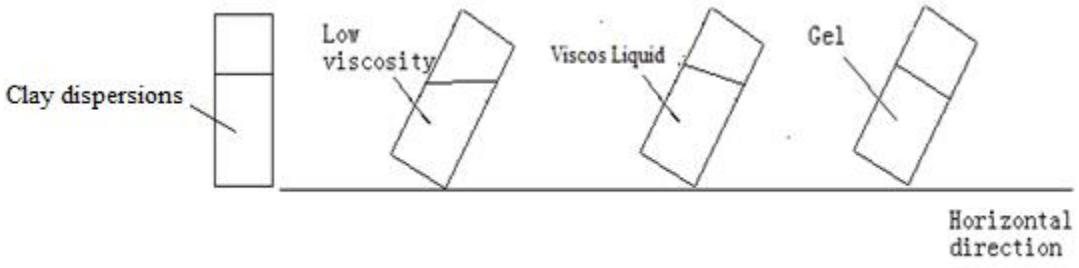

Figure 7 Examples of sample behavior during an inverted tube test that was use to assess the sample rheology.

This interaction can be affected by for example pH, particle and salt concentration. As Figure 8 illustrates, samples with low viscosity readily flow while samples with higher viscosity will flow more slowly, while gels will not flow at all [46].

3.3 Resistivity measurements

The resistivity of gels can be used as a measure of the tortuosity of the pores in the material. Comparing porous materials of the same dry weight concentration, a higher resistance is an indication that the electron need to travel a longer path (higher material tortuosity) than if the resistance was lower. Such effects can be expected in samples with clay particles that have different orientation relative the direction of the resistivity measurement. However, different type, concentration and distribution of clay will affect the resistivity. This will also be the effect of different solvent type and salt concentration. However, by keeping all parameters constant except the clay orientation, an estimation of the change in tortuosity can be made [47].

4 Experimental methods

4.1 Methods used for the clay – urea/urease system

4.1.1 Clay preparation

Exfoliated clay sols were fractioned into various sizes fractions by the following process that have been described earlier [7]. First, the greenish colored clay lumps were ground to powder in a crucible. The clay powder was suspended in a 1M of NaCl (Sigma, Sweden) and the suspension was ultra-sonicated using an ultrasonic probe (Viber-cell 505, Sonics, USA) with an amplitude of 40% for 150 seconds. After leaving the sample to rest for 30 min the suspension were ultracentrifuged (Optima XL-100K ultracentrifuge with 90 Ti rotor, Beckman Coulter, Palo Alto, CA, USA) at 35000×g for 90 min. The pellet was re-dispersed in salt solution again and then centrifuged. The centrifugation and redispersion was repeated in total 3 times to exchange as many of the ions associated with the clay surfaces to sodium ions. The collected pellet after the last centrifugation was re-dispersed into 250 ml of MilliQ water, and to remove excess salt the dispersion was dialysed (MWCO 12-14000 kDa, Sigma-Aldrich, USA) against deionised water until the conductivity did not change anymore. The suspension was left to sediment for 3 days in Imhoff cones to remove impurities like iron oxide and feldspar. The dispersion was then centrifuged at 7000×g and then 17000×g for 90 min to get size fraction 1 and 2, respectively. Fraction 2 was the fraction used for all experiments with clay in this thesis. The nontronite clay sheets have an average particle length of 372 nm and width of 146 nm, as previously reported [48]. Dry weight measurements were made to find the clay concentration of the fraction 2 pellets. The density of the nontronite clay particles is around 3 g/cm^3 [11].

4.1.2 Sample formulation

The phase behavior at different clay and salt concentrations were investigated after the

following sample formulation. Fraction 2 nontronite clay pellet was mixed with urea solution (Sigma, Sweden), MilliQ water (Millipore MilliQ, 18 MΩ cm) and urease enzyme solution. Homogenous gelation of the samples was achieved by *in situ* formation of NH_4HCO_3 salt, through hydrolysis of urea (Sigma) by the enzyme urease (Sigma, Jack Bean-urease type IX, Specific activity ~75,000 U/g). The enzyme concentration in all samples was 1.5 mg/ml [49]. The mixing of the different sample constituents was made in 1.5 ml Eppendorf tubes (Eppendorf AG German). The total sample volume in the finished samples was 0.5 ml. After vortexing the sample dispersion for about 10 seconds it was transferred into 5 mm NMR tubes and capped after which it was left to gel for a few days.

4.1.3 Sample imaging, magnetic alignment and optical birefringence observations

Samples were imaged between crossed polarizers both before and after magnetic field exposure to a NMR spectrometer magnetic field (11.7 Tesla) for 5 min. Imaging of the samples were made approximately 40 seconds after taking samples out of NMR which for some samples at lower clay concentration resulted in relaxation of the induced alignment. The samples were then imaged without crossed polarizers.

4.1.4 Resistivity measurements

The resistivity was measured before and after magnetic exposure with a digital multimeter (Agilent 34401A, Agilent Technologies, Palo Alto, USA) together with copper wires as shown in Figure 8. From the resistivity the conductivity could calculated. The copper wire was inserted 1-2 mm both at the top and bottom of the sample before recording the resistivity.

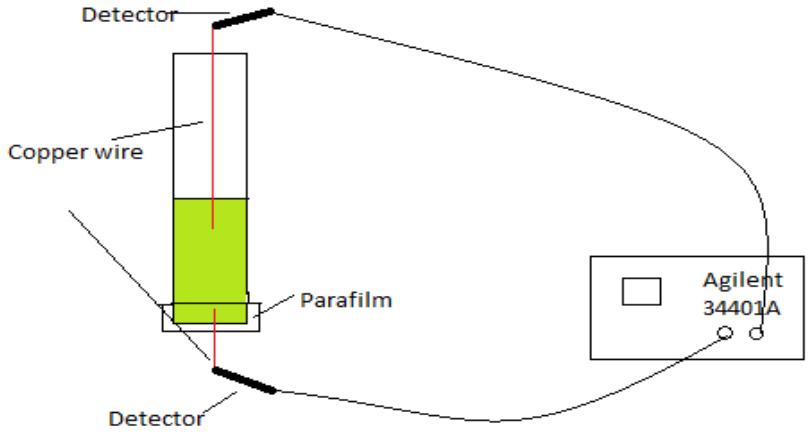

Figure 8 Resistivity measurement set-up.

4.2 Results

As earlier mentioned these studies aimed at investigating the influence of clay and salt concentration on the magnetic alignment of the clay sheets. Several other relevant characterization methods were also used and the results from these experiments are presented below.

4.2.1 Clay – urea/urease system

Figure 9 shows the sample appearance without crossed polarizers at different clay and salt concentration. Figure 10 and 11 show the same samples viewed between crossed polarizers before and after magnetic exposure. In Figure 10 and 11 the samples have exactly the same composition, however, the samples in Figure 10 has been used for resistance measurements where the insertion of the electrodes mechanically disturb mainly the upper surface of the sample. To control for this the samples in Figure 11 were made as these have not been used for resistance measurements.

4.2.2 Phase behavior - Color differences, aggregates and crack formation

Figure 9 to 11 clearly show color difference going from transparent to yellow-green when increasing the clay and salt concentration. The higher clay and salt concentration, the more colored the sample appears to be. At 0.8 vol% clay concentration the largest change in color takes place between at a salt concentration between 10 and 1 mM. In Figure 10 the two samples with 0.8 vol% clay and 0.1-1 M salt had small birefringent regions inside the samples before magnetic exposure. These disappear almost completely after magnetic exposure. Cracks are apparent in the sample with 0.1 vol% clay and 1M salt in Figure 11, but not in Figure 10 even though the samples have the same composition.

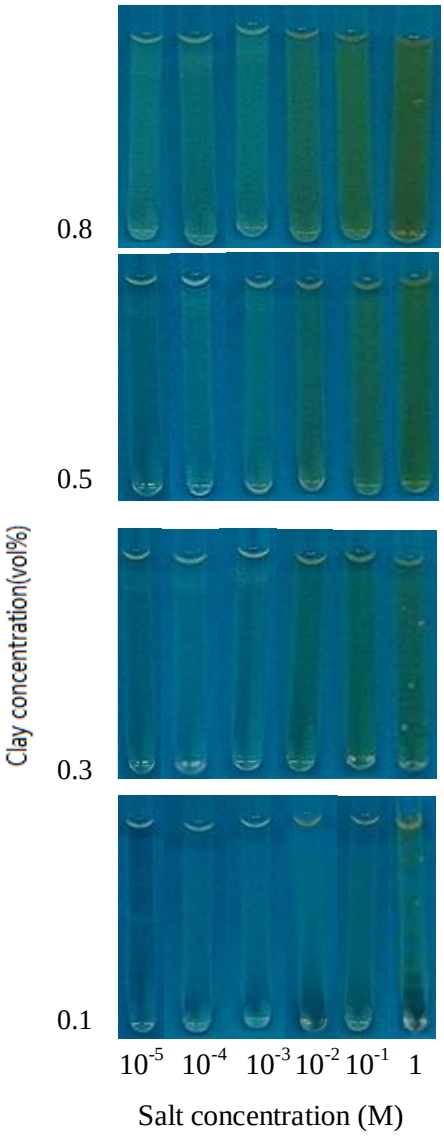

Figure 9 Images of samples taken without crossed polarizers after magnetic field exposure.

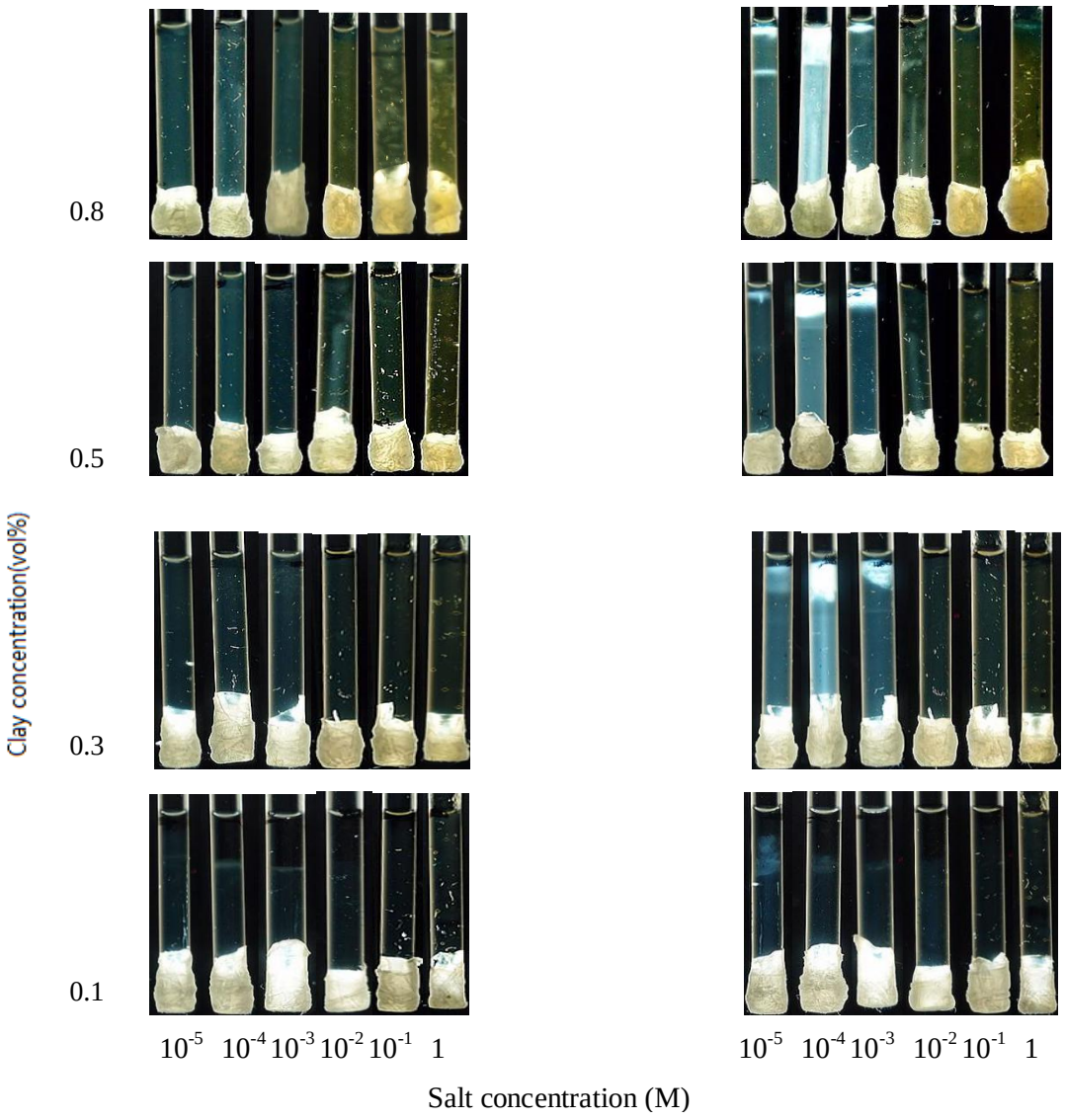

Figure 10 Samples with varied clay and salt concentration. This is the first sample series imaged between crossed polarizers before (left) and after magnetic exposure (right side).

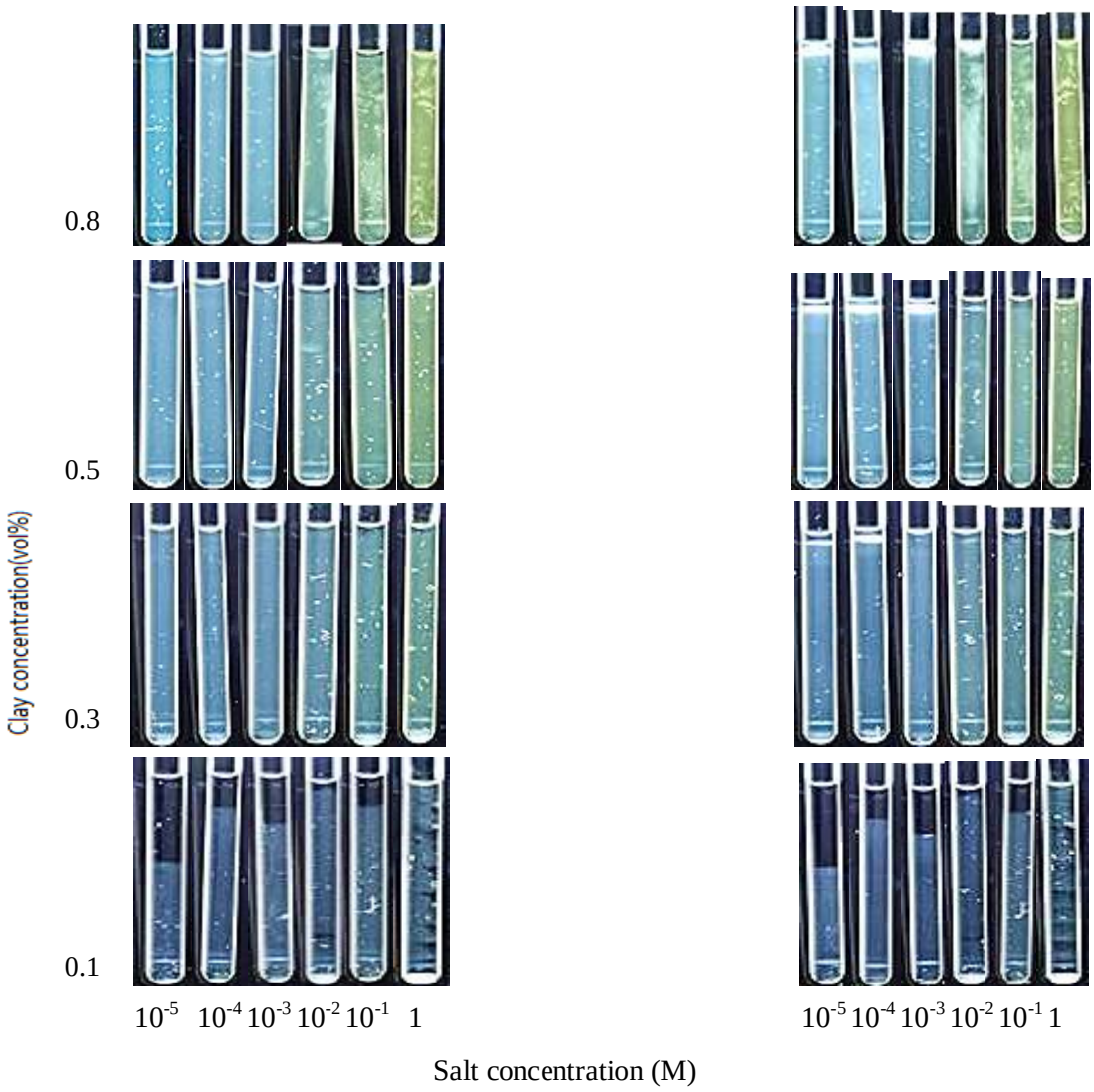

Figure 11 Sampled with varied clay and salt concentration. Second sample series imaged between crossed polarizers before (left) and after magnetic exposure (right side).

4.2.3 Sample rheology and phase separation

After magnetic exposure an inverted tube test was performed. The result from this test can be viewed in Table 1 where it is apparent that higher clay and salt concentration leads to more viscous samples, or even gelation. As one moves from the lower left to the upper right corner the samples goes from a liquid state with loose flocculates, to viscous samples where some have flocculated/phase separated. At the highest salt concentration all samples had gelled. Flocculation and phase separation is more common at lower salt concentration. Still, the phase separation is undoubtedly most pronounced at a clay concentration of 0.1 vol% with low to moderate salt concentration.

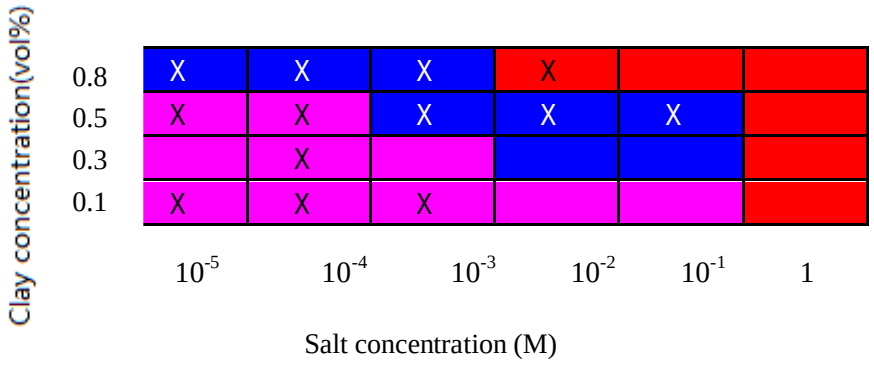

Gel	
Viscous liquid	
Liquid	
Phase separated	X

Table 1 Phase behavior of samples after magnetic alignment.

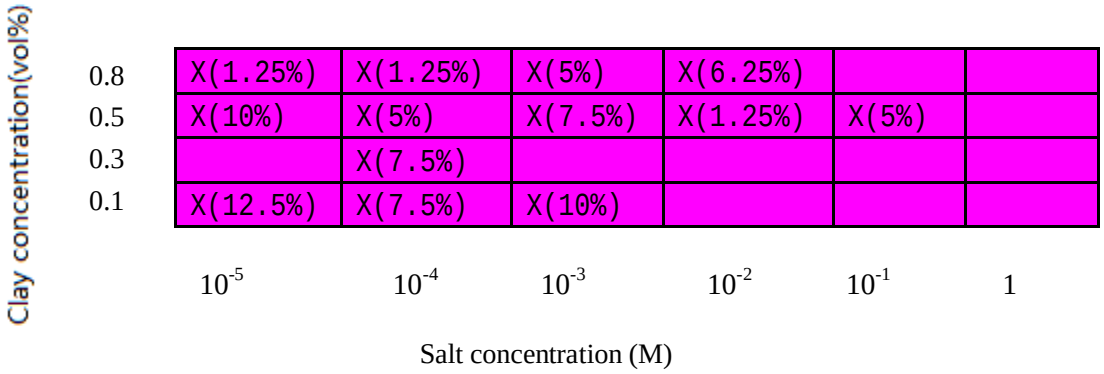

Dispersion	
Phase separated	X

Table 2 Degree of phase separation in samples. The percentages represents the relative size (length) of the upper phase relative the total sample size (length) in the samples that phase separated.

Table 2 indicates the degree of phase separation in the samples. The total length of each sample was 40 mm.

4.2.4 Magnetic alignment and optical birefringence

Figure 10 will be the figure that is most discussed in relation to the magnetic alignment as the images in Figure 11 suffers from the presence of unpolarized light , due to light leaking in during the experiment. It is therefore hard to see any difference in birefringence before and after magnetic exposure in Figure 11.

Figure 10 shows that magnetic exposure of the samples causes them to display birefringence at a clay concentration of 0.3 vol% and above if the salt concentration is bellow 10 mM. There are hints of weak birefringence is some of the samples with 10mM salt. Also worth nothing is the very strong birefringence found on top of the some samples after magnetic exposure in both Figure 10 and 11. No birefringence was observed in the samples with 0.1 vol% clay before or after magnetic exposure.

4.2.5 Resistivity measurements

The resistivities of the samples were tested to see how the alignment of the clays would affect the samples resistance. The resistivity was only measured in a few samples because the fluctuations in the resistivity values of the same samples were very large. Figure 12 display the resistivity of samples with a constant clay concentration of 0.8 vol%, and a varied salt concentration. For almost all samples the resistivity decreased after magnetic alignment. Nevertheless, the change is so large that it is unlikely to be related to a change in the clay orientation. Instead it might be related to salt formation from the copper wire during the measurements. Such salt formation can be seen as a for copper salts typical blue colored hue, on the top of the sample with 0.8 vol% clay and 1M salt in Figure 12.

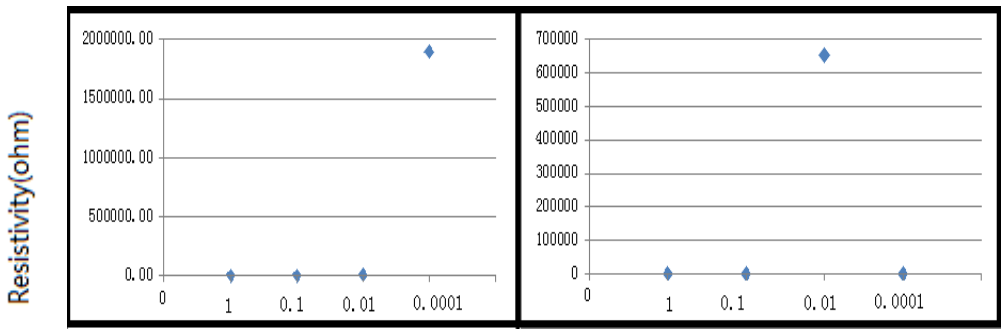

Figure 12 The measured resistivity of the samples before and after magnetic alignment. The salt concentration of the four samples were 1, 10^{-1}, 10^{-2} and 10^{-4} M, at a constant clay concentration of 0.8 vol%.

4.2.6 Latex/clay composite

This part of the work aimed to formulate a new latex-clay composite films to study the effect of clay alignment in the film on the film permeability.

The mean latex particle sizes were measured in the latex sols are presented in Table 3 and Figure 13. The mean particle size for the different latexes ranges between 102 to 126 nm.

Latex type	PX9612	PX9272	PX9704	PX9340
Mean particle diameter (nm)	115.3	126.9	102.0	109.0
Polydispersity	0.057	0.005	0.005	0.005

Table 3 The mean particle diameter and the polydispersity of the 4 different latex types.

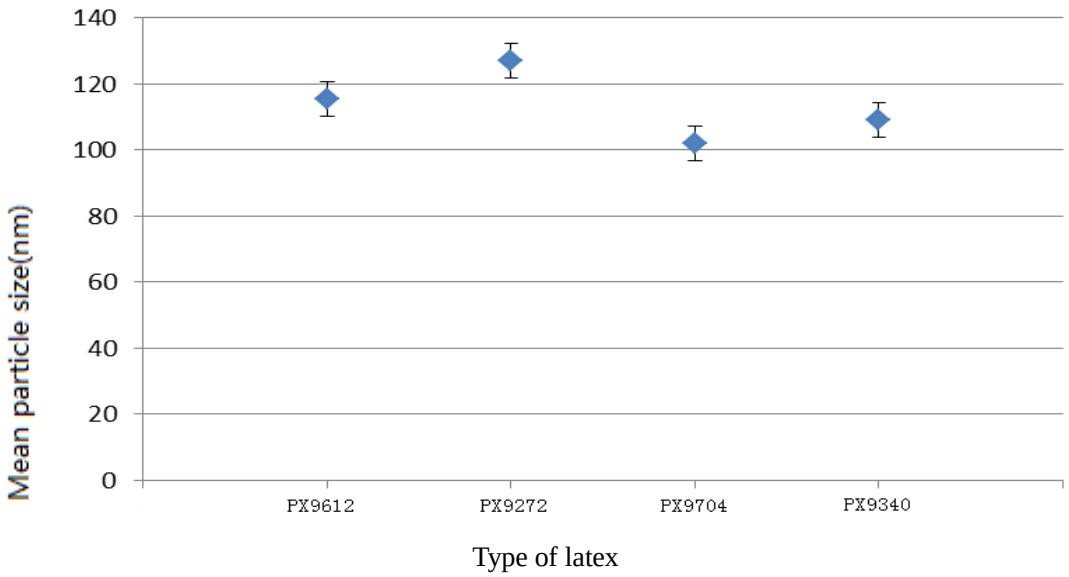

Figure 13 Mean particle sizes for four different latex types as measured with dynamic light scattering.

4.2.7 Destabilization of latex dispersions with urea/urease method.

The phase behavior of different latex types, concentrations and salt concentrations are displayed in Table 4-7. As can be seen no samples gelled with the urea/urease destabilization, which was a requirement before trials with added clay would be attempted. Hence the urea/urease destabilization method was abandoned and instead the glucono-δ-lactone/$CaCO_3$ method was tried.

Dispersion	
Phase separated	X

Salt (M)	15	20	25	30
1			X	X
0.5		X	X	X
0.2				
0.05				X

Latex(%)

Table 4 The phase behavior for Latex PX9272 with urea/urease destabilization.

Salt (M)	15	20	25	30
1				
0.5		X	X	X
0.2		X	X	
0.05		X	X	

Latex(%)

Table 5 The phase behavior for Latex PX9612 with urea/urease destabilization.

Salt (M)	15	20	25	30
1			X	X
0.5		X	X	X
0.2				
0.05				X

Latex(%)

Table 6 The phase behavior for Latex PX9704 with urea/urease destabilization.

Salt (M)	15	20	25	30
1			X	X
0.5	X	X	X	
0.2		X	X	
0.05		X	X	X

Latex(%)

Table 7 The phase behavior for Latex PX9340 with urea/urease destabilization.

4.2.8 Destabilization with the glucono-δ-lactone/$CaCO_3$ method

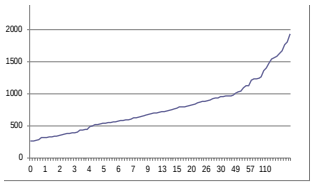

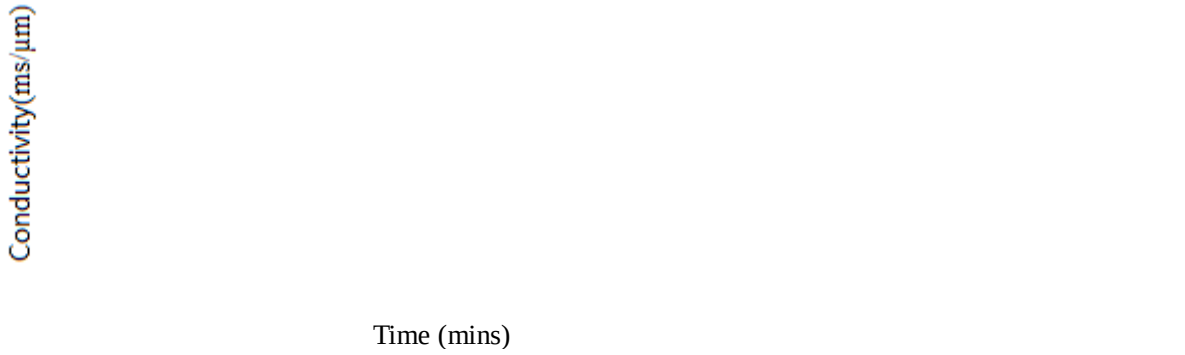

Figure 14 Conductivity of an aqueous dispersion of $CaCO_3$ and glucono-δ-lactone over time.

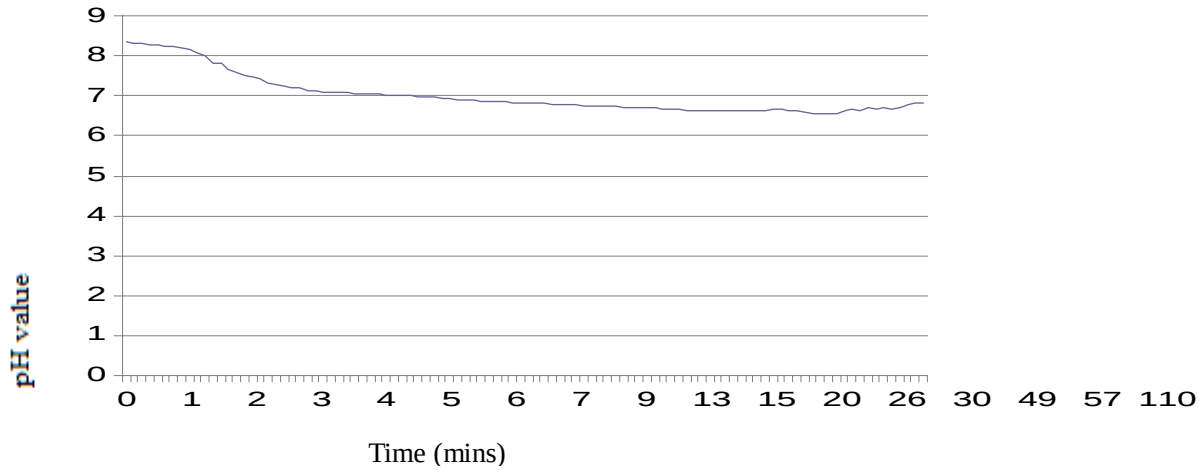

Figure 15 pH value of an aqueous dispersion of $CaCO_3$ and glucono-δ-lactone over time.

The pH and conductivity was measured over time for a dispersion of $CaCO_3$ and glucono-δ-lactone as shown in Figure 14 and15. The conductivity changed more quickly than the pH. The pH decreased from pH 8.5 to 7 in 5 minutes and did not decrease more over time. The dispersion of initially insoluble $CaCO_3$ was totally transparent after 170 min. The conductivity on the other hand increased during the whole measurement.

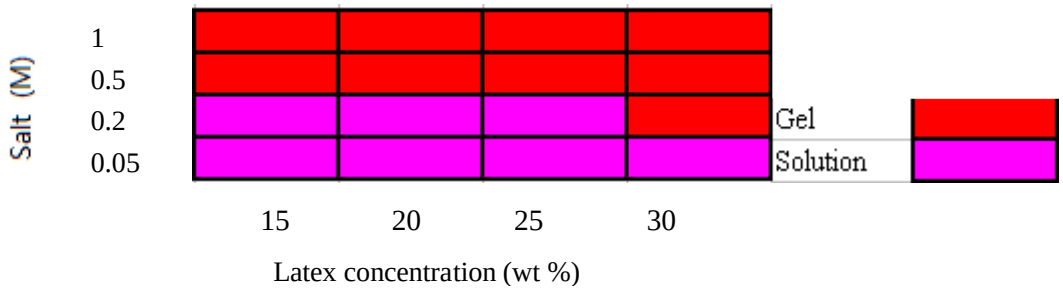

Table 8 The phase behavior of $CaCO_3$/ glucono-δ-lactone and latex.

Several samples gelled in Table 8 and to find such samples was the goal of this particular experiment. Even so, the gelation the samples were not reproducible which was why also this method of latex sol destabilization was abandoned. Instead all time was spent on investigating the phase behavior of only nontronite clay at different clay and salt concentrations.

5 Discussion

Except from being used in nanocomposites, clay dispersions and their rheological properties are of great importance in many industrial applications. The focus of this thesis discussion will be put on how the nontronite clay and salt concentration affect the magnetic alignment and the rheological properties. Phase behavior characterizations of different sample properties have indeed produced some very interesting results. Resistivity measurements were also attempted, however the validity of those measurements for the study of the clay microstructure is questionable. Also the formulation of a latex/ clay composite for studies of liquid permeability though magnetically aligned latex/clay composites failed. The reason that the failed results from the formulation of the latex/clay composites are still included in the thesis is to provide a record of these studies as they took up a considerable time of the practical thesis work.

5.1 Sample color and rheology as a function of clay and salt concentration

Figure 9 show that all samples with a clay concentration above 0.1 vol% transitioned from a transparent to a yellow-green appearance as the salt concentration were increased from 1 to 10 mM NH_4HCO_3. At constant clay concentration the sample where more colored at a higher salt concentration. The reason for this is likely to be the difference in pH between the samples (not measured). Urease first produces ammonia from the urea which increases the pH until the buffering pH of 9.3 is reached [7]. At the buffering pH the NH_4HCO_3 salt will be formed. The pH is known to influence the oxidation state of the iron ions present in clay sheets which explains the color differences at constant clay concentration [50]. The reason for the decrease in color intensity of the samples with decreasing clay concentration at a constant salt concentration is that the colored clay particles and their colored ions become more dilute. Interestingly the colored samples are roughly the same samples that are defined as gels in

Table 1. This makes sense as the most colored samples have the highest salt concentration and salt is known to cause gelation in clay dispersions [11].

5.2 Magnetic alignment and rheology

Except for the 0.1 vol% sample, Figure 10 show magnetic alignment in all samples with a salt concentration below 10 mM. To find the relationship between magnetic alignment and clay and salt concentrations was an important goal of this thesis. Hence, under the conditions used in this study, clay concentration does not determine which sample that can align. Instead salt concentration is the decisive factor. It should be noted that the samples with 10^{-5}M salt in Figure 11 have less birefringence than the samples with 10^{-4}M salt. One possible reason could be that the clay dispersions with a salt concentration of 10^{-5} M relax faster than at 10^{-4}M. As the samples needed to be moved from the NMR magnet after alignment, their birefringence relaxed partly. Abrahamsson and co-workers observed no magnetic alignment in a 0.5 vol% nontronite clay gel gelled with 1M urea with the addition of urease, which is consistent with the results in this thesis [7]. If one compares the inverted tube test observations in Table 1 with the magnetic alignment results in Figure 10, it becomes apparent that the rheological properties are poor predictors of which samples that magnetically align or not. This is especially evident at low clay concentration.

The presence of birefringent 'flocs' can be seen at a clay concentration of 0.8 vol% and 0.1-1M salt concentration. This type of birefringence has previously been observed by Abrahamsson and colleagues [7] and they theorized that the birefringent flocs actually consisted of local regions of collectively aligned clays that were birefringent. These birefringent regions might have formed during sample mixing which could cause flow birefringence. It is then possible that the slow salt formation locked the orientation of the clays into this locally aligned state. Phase separation was clearly observed at a clay concentration of 0.1 vol%, but no birefringence could be observed. Hence these samples are phase separated, yet not ordered by the magnetic field.

Figure 10, 11 and 16 show how regions at the top of some of the samples form a thin but intensely birefringent phase after clay alignment. A schematic with the different phases illustrated can be found in Figure 16. The birefringent phase appears in the middle of two isotropic or less birefringent phases. One hypothesis is that a secondary phase separation formed a nematic phase from residual clay particles present in the upper isotropic phase. This upper isotropic phase would have been formed after an earlier primary phase separation that formed two isotropic clay phases of different clay concentration. This could be confirmed in the future by SAXS measurement on these phases. Except SAXS measurements it would be useful to determine to the dry weight concentration of the different phase separated layers as this could shine more light on which phases that are present.

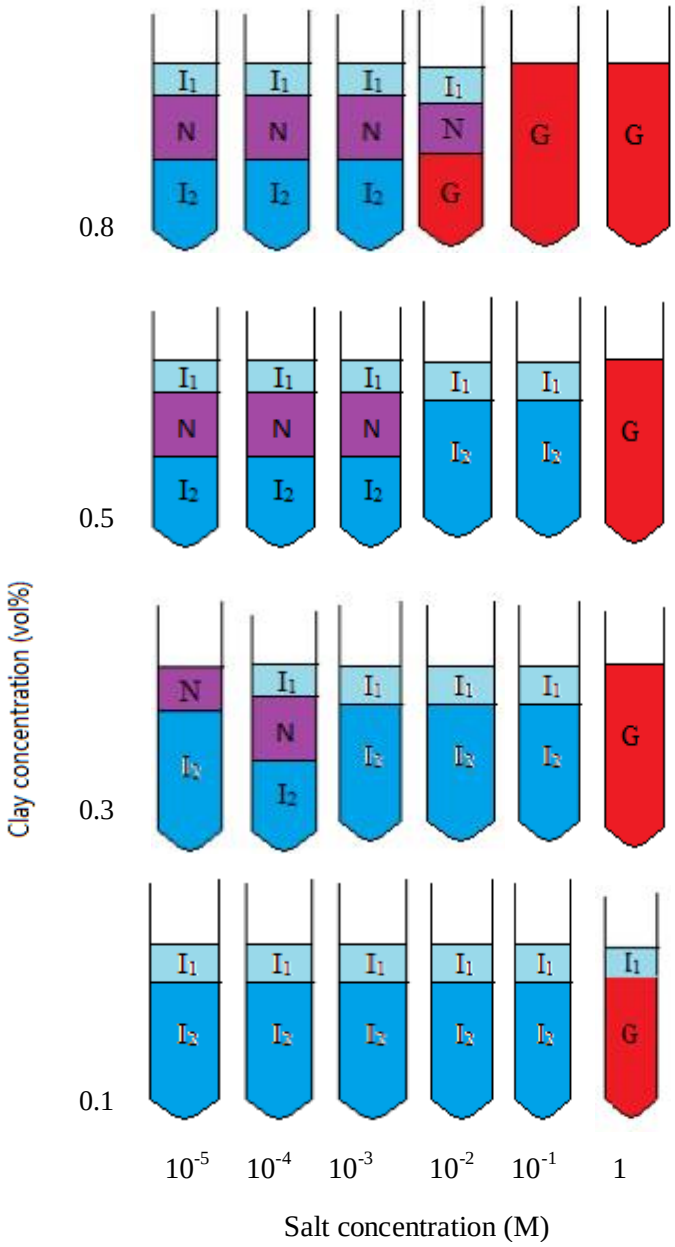

Figure 16 Observed phase separation at varied clay and salt concentration. $I_{1,}$ $I_{2,}$ N and G stand for isotropic phase, nematic-like phase and gel phase, respectively. I_1 stand for isotropic low clay concentrations and I_2 stand for isotropic higher clay concentrations.

Table 1 shows that the samples gel at a high salt and clay concentration and as expected there is a viscous liquid region between the liquid and gel region. Michot and collegues have reported that nontronite clay disperions with a clay concentration of 0.83 vol% and no salt gelled due to the close packing of the system. They also showed that when salt was added gelation took place down to a clay concentration of 0.3 vol%, when the salt concentration was around 10^{-2} M NaCl. Compared to Michot's results phase separation is in this work seen over

a much larger range of clay concentrations [11]. This might be because the addition of enzyme and the use of another type of salt in this study.

5.3 Resistivity measurements

As mentioned earlier the resistivity measurements are not expected to be accurate as the resistivity measured in the samples fluctuated a lot. Also, copper ions dissolved in the sample during measurements which of course increased the conductivity of the samples. Still, differences in conductivity because of clay orientation would be expected if a more stable measurement set-up would have been used. Fukue and co-workers measured the resistivity of clay containing materials and related the conductivity to concentration of ions and counter ions next to the surface of clay particles, water content and even the orientations of the water molecules in the region of the electric double layer [51]. It has also been shown that the resistivity increased at a higher clay concentration. In the summary, no conclusion can be drawn based on the resistivity measurements in this thesis. Still, literature indicate that the ionic strength and clay type/concentration could have major influence on the resistivity of the dispersions [52].

5.4 Latex/clay composite

The goal of these formulations experiments were to make latex/clay films that could be used to study the permeability of films containing clays with different clay orientation. However, both the destabilization with urea/urease and $CaCO_3$/glucono-δ-lactone proved unsuccessful in the effort to reproducibly produce mechanically stable films. The $CaCO_3$/glucono-δ-lactone method did form gels, however, even when repeatedly testing the mixing of the same sample recipe the gelation of the sample failed in many cases without any obvious explanation. Hence this gelation method was abandoned. One theory for why it was so hard to form gels was that the large surface area of the sol buffered changes in pH or that the latex particles adsorbed the urease enzyme on its surface so that it became inactive, effectively hindering salt formation and gelation. All latex phase behavior diagrams show phase separation. This might be caused by insufficient salt concentration for reasons mentioned above or that the change in pH caused by the *in situ* gelation methods instead favor flocculation.

6 Conclusions

To find the relationship between magnetic alignment, and clay and salt concentration were important goals of this thesis. In this study it was found that clay concentration does not determine which sample that can align, instead salt concentration was the decisive factor. At a salt concentration of 10^{-3} NH_4HCO_3 and below the samples could align in an 11.7 Tesla magnetic field, but not above this salt concentration. Also, the rheological properties were poor predictors of which samples would magnetically align. It is therefore not possible to say that a more viscous clay sample will align slower than a less viscous sample.

7 Future work

Further studies of how the magnetic alignment would be affected by different magnetic field strength would be interesting. Also, SAXS measurements would be beneficial to prove the existence of nematic phase in some of the samples. Furthermore, birefringence relaxation time and rheology measurements would also be of use as these would quantitatively determine the clay dynamics of the system. Also, it would be beneficial to measure the pH of all the samples in the phase diagram, as pH can have large influence on the phase behavior of clay containing systems.

8 Reference

1. EuStis S., EL-Sayed M.A., Why gold nanoparticles are more precious than pretty gold Noble metal surface plasmon resonance and its enhancement of the radiative and non radiactive properties of nanocrystals of different shapes, Chemistry Society Review, 35, p.209-217 (2005)

2. Valiev R., Material science: Nanomaterial advantage, Nature ,419, p.887-889 (2002)

3. Wang J., Nanomaterial-based electrochemical biosensors, Analyst, 130, p.421-426 (2005)

4. Glotzer S.C, Solomon M.J., Anisotropy of building blocks and their assembly into complex structures, Nature Materials, 6, p.557-562 (2007)

5. Wang Y.C., Huang T.K., Tung S.G., Self-assembled clay films with a platelet-void multilayered nanostructure and flame-blocking properties, Scientific reports, 3, 2631, p.1-6 (2013)

6. Luo J.J., Daniel I.M.., Characterization and modeling of mechanical behavior of polymer/clay nanocomposites, Composites Science and Technology, volume 63, issue 11, p.1607-1616 (2003)

7. Abrahamsson C., Nordstierna L., Bergenholtz J., Nyden M., Magnetically induced structural anisotropy in binary colloidal gels and its effect on diffusion and pressure driven permeability., Soft matter, 24, 10, p.4403-4412 (2014)

8. Camerel F., Gabriel J.-C.P., Batail P., Magnetically induced large mesoporous single-domain monoliths using a mineral liquid crystal as a template, volume 13, issue 5, p. 377-381 (2003)

9. Mitsunaga M., Ito Y., Ray S.S., Okamoto M., Intercalated Polycarbonate/Clay Nanocomposites: Nanostructure Control and Foam Processing, Macromolecular Materials and Engineering, volume 288, issue 7, p. 543 -548 (2003)

10. Bharadwaj R.K., Modeling the barrier properties of polymer-layered silicate nanocomposite, Macromolecules,volume 34, number 26, p.9189-9192 (2001)

11. Michot L.J., Bihannic I., Maddi SS. Funari S.S., Liquid- crystalline aqueous clay suspensions, Proceedings of the National Academy of Sciences, volume 103, number 44, p.16101-16104 (2006)

12. Maitland G.C., Oil and gas production, Current opinion in Colloid & Interface Science, volume 5. issue 5-6, p.301-311 (2000)

13. Petrucci R.H., Harwood W.S., General chemistry: principle and modern applications. 9th ed. (2007)

14. Russel W., Saville D.A., Schowalter W.R., Colloidal Dispersions, Cambridge University press, p.12 (1989)

15. Adamson A.W., Gast A.P., Physical chemistry of surfaces, 6th edition, p.169 (1967)

16. Binks B.P., Horozov T.S., Colloidal particles at liquid interfaces: An introduction. Cambridge University Press, p.1-10 (2008)

17. Onsager L. The effects of shape on the interaction of colloidal particles, Annals New York Academy of Science**,** p.627-659 (1949)

18. Chi E.Y., Krishnan S., Roles of conformational stability and colloidal stability in the aggregation of recombination human granulocyte colony-simulating factor, volume 12, issue 5, p. 903-913 (2003)

19. Fleer G.J., Lyklema J., Polymer adsorption and its effect on the stability of hydrophobic colloids, Journal of colloid and interface science,volume 46, number.1, p1-12 (1974)
20. Islam M.A., Einstein-Smoluchowski Diffusion equation: a discussion, Physica Scripta volume 70, 120-125 (2004)
21. Bates T.F., Bradley W.F., Plummer N., Waxman M.H., Weaver C.E., Clay and clay minerals on clays and clay minerals. p.21 (1956)
22. Goodwin J.W., Colloidal dispersions, The Royal Society of Chemistry, Burlington House, London W1V OBN, University of Bristol 10^{th} , p.9-40 (1981)
23. Ohshima H., Biophysical Chemistry of Biointerfaces, John Wiley & Sons, Inc , Hoboken, NJ, USA, p.420 (2010)
24. Guo D., Mechanical properties of nanoparticles: basics and applications, Journal of Physical D: Applied Physics (2014)
25. Badawy A., Luxton T., Silva R., Scheckel K., Suidan M.., Tolaymat T., Impact of environmental conditions (pH, Ionic Strength, and Electrolyte type) on the surface charge and aggregation of silver nanoparticles suspensions, Environment Society Technology. 44, p.1260-1266 (2010)
26. Schmitz K., Macro ions in solution and colloidal suspension, Department of chemistry. University of Missouri-Kansas City (1992)
27. Dunn J.R., Hudec P.P., Water, clay and rock soundness, The Ohio journal of science, volume 66, issue 2, p.153-168 (1966)
28. Torrence M.R., Adsorbed water on clay: A review, M.I.T. Soil engineering. Cambridge, Massachusetts (1960)
29. Marshall C.E., Krinbill C.A., The clay as colloidal electrolytes, Journal of Physical Chemistry, p.1077-1090 (1942)
30. Tombacz E., Szekeres M., Colloidal behavior of aqueous montmorillonite suspensions: the specific role of pH in the presence of indifferent electrolytes, Applied clay science, volume 27, issue 1-2, p.75-94 (2004)
31. Mullins C.E., Magnetic susceptibility of the soil and its significance in soil science - a review, Journal of soil science, volume 28, issue 2, p.223-246 (2006)
32. Tang B.Z., Geng Y.H., Lam J.W., Li B., Processible nanostructure materials with electrical Conductivity and Magnetic Susceptibility: Preparation and Properties of Maghmite/Polyaniline Nanocomposite Films. Chemistry Mater, volume 11, p.1581-1589 (1999)
33. Wiese G.R., Healy T.W., Effect of particle size on Colloid Stability, Transamination Faraday Society, p.490-499 (1970)
34. Skipper N.T, McConnell R., Computer simulation of interlayer water 2:1 clays, Journal of Chemistry Physics, 94, p.7434 (1991)
35. Grim, R.E., Clay Mineralogy, 2nd edition, p.10 (1968)
36. Te Nijenhuis K., Thermoreversible networks, Advanced Polymer Science, 130, p.1-267 (1997)
37. Clark A.H., Gels and gelling, Physics chemistry of food. p.263-305 (1992)
38. Zhang Z.X., Duijneveldt J.S., Isotropic-nematic phase transition of nonaqueous suspensions of natural clay rods, Journal of chemical physics 124, number15, 154910 (2006)
39. Dijkstra M., Hansen J.P., Madden P.A., Gelation of a clay colloid suspension, Physics

Review Letter volume 75, number 11, p.2236 (1995)
40.Abend S., Lagaly G., Sol–gel transitions of sodium montmorillonite dispersions, Applied Clay Science, 16, p.201-227 (2000)
41. Schofield R., Samson H., Discussions of the Faraday Society, 18, p.135-145 (1954)
42. Sprokel G.J., Birefringent liquid crystal structure, United State Patents (1975)
43. Robinson C., Liquid-crystalline structures in polypeptide solution, Tetrahedron, vol 13, p.219-234 (1961)
44. http://hyperphysics.phy-astr.gsu.edu/hbase/phyopt/polcross.html [Accessed on: January 14, 2014]
45. Gupta D, Tator C.H., Shoichet M.S. Fast-gelling injectable blend of hyaluronan and methylcellulose for intrathecal, localized delivery to the injured spinal cord, volume 27, issue 11, p.2370-2379 (2006)
46. Ganji F., Abdekhodaie M.J., Gelation time and degradation rate of chitosan-based injectable hydrogel, J Sol-Gel Society Technology, p.42:47-53 (2007)
47. Lima O.A., Sharma M.M., A grain conductivity approach to shaly sanstones, Geophysics, 55(10), p.1347-1356 (1990)
48. Ramiasa M., Locock K., Abrahamsson C., Nyden M., Smart polymer-clay composite nanomaterials, Manuscript (2014)
49. Qin Y. and Cabral J. M., Kinetic studies of the urease-catalyzed hydrolysis of urea in a buffer-free system, Applied biochemistry and biotechnology, 1994, 49, p.217-240 (2000)
50. Temple K.L. and Colmer A.R., The Autotrophic oxidation of iron by a new bacterium: Thiobacillus ferrooxidans, J. Bacteriol, 62(5), p.609 (1951)
51. Fukue M., Minato T., The micro-structures of clay given by resistivity measurements, volume 54, issues 1-2, p.43-53 (1999)
52. Yoon G.L., Park J.B., Sensitivity of leachate and fine contents on electrical resistivity variations of sandy soils, Journal of Hazardous materials, volume 84, issue 2-3, p.147-161 (2001)